

# A note on non-flat points in the $SU(5) \times U(1)_{PQ}$ F-theory model

Ismail Achmed-Zade,<sup>a,b</sup> Iñaki García-Etxebarria<sup>c,1</sup> and Christoph Mayrhofer<sup>a</sup>

<sup>a</sup>Arnold Sommerfeld Center for Theoretical Physics,  
Theresienstrasse 37, 80333 München, Germany

<sup>b</sup>Max-Planck-Institut für Physik,  
Föhringer Ring 6, 80805 München, Germany

<sup>c</sup>Department of Mathematical Sciences, Durham University,  
Durham, DH1 3LE, United Kingdom

E-mail: [I.AchmedZade@physik.uni-muenchen.de](mailto:I.AchmedZade@physik.uni-muenchen.de),  
[inaki.garcia-etxebarria@durham.ac.uk](mailto:inaki.garcia-etxebarria@durham.ac.uk),  
[christoph.k.mayrhofer@gmail.com](mailto:christoph.k.mayrhofer@gmail.com)

**ABSTRACT:** Non-flat fibrations often appear in F-theory GUT models, and their interpretation is still somewhat mysterious. In this note we explore this issue in a model of particular phenomenological interest, the global  $SU(5) \times U(1)$  Peccei-Quinn F-theory model. We present evidence that co-dimension three non-flat fibres give rise to higher order couplings in the effective four-dimensional superpotential — more specifically, in our example we find **10555** couplings.

**KEYWORDS:** F-Theory, Superstring Vacua, Brane Dynamics in Gauge Theories

**ARXIV EPRINT:** [1806.05612](https://arxiv.org/abs/1806.05612)

<sup>1</sup>Formerly at Max-Planck-Institut für Physik, Föhringer Ring 6, 80805 München, Germany.

---

**Contents**

<b>1</b>	<b>Introduction</b>	<b>1</b>
<b>2</b>	<b>The geometric setup</b>	<b>3</b>
2.1	Fibre geometry at the non-flat points	6
<b>3</b>	<b>Fluxes</b>	<b>8</b>
3.1	The second Chern class	9
3.2	U(1)- and matter surface fluxes	10
3.3	Second Chern class of the $SU(5) \times U(1)_{PQ}$ fourfold	10
<b>4</b>	<b>The weak coupling limit and the IIB picture</b>	<b>11</b>
4.1	Weak coupling limit	11
4.2	Ext groups and quiver theory	14
4.2.1	Non-commutative crepant resolution of the conifold	14
4.2.2	The non-flat point at weak coupling	18
<b>5</b>	<b>The mirror picture</b>	<b>20</b>
<b>6</b>	<b>Conclusions</b>	<b>22</b>
<b>A</b>	<b>6d anomaly cancellation</b>	<b>23</b>
A.1	Counting charged hyper multiplets	23
A.2	Counting uncharged hyper multiplets	25

---

**1 Introduction**

F-theory [1] models have been extensively studied in the last few years, starting with [2–6], for their promising features for GUT-inspired string theory model building.

A detailed analysis of such models reveals that they sometimes develop “non-flat” points: these are points on the base over which the dimension of the fiber jumps and, therefore, the standard M-/F-theory [1, 7] is not directly applicable.<sup>1</sup> In most phenomenological F-theory models, where such loci would appear in the generic setting, they are excluded from consideration by restricting the analysis to a highly non-generic setup.

The goal of this note is to address the physical implications of such non-flat point if they appear *at co-dimension three* [8]. We will not give a general solution, but rather analyze in detail a particular example with interesting phenomenological properties. All the explicit details that we work out in this article are obtained for the  $SU(5) \times U(1)$  Peccei-Quinn

---

<sup>1</sup>Examples of the appearance of such points in the literature go back to the early days of F-theory [8] and showed up again with the advent of the intense study of non-abelian gauge groups together with U(1) selection rules [9, 10]. For instance, two of the many examples appeared in the context of  $SU(5)$ -top constructions over  $\mathbb{P}_{[1,1,2]}$  [10–12].

model which was already studied in [13–15], and follow-up works, and which we review in detail below. However, we expect related models to be amenable to an analysis akin to the one we perform here.

Our main result is that in the weak coupling limit these non-flat points do not interfere with the desirable GUT-physics, so they are harmless for model building purposes. Indeed, the non-flat points occur at special (self-)intersection points of the matter curves. As we show, they lead to higher order coupling built from the matter states related to the (self-)intersecting curves. In our example at hand, the  $\mathbf{10}_3$  curve meets the triple self-intersection of the  $\mathbf{5}_{-1}$  curve such that we observe a  $\mathbf{10}_3\mathbf{5}_{-1}\mathbf{5}_{-1}\mathbf{5}_{-1}$ -coupling. The presence of this coupling will not spoil the physics in a successful  $SU(5)$  GUT model. In fact, they will have very little effect, since the modes involved will typically be massive.<sup>2</sup>

Before going into the analysis of non-flat points in our example, we will resolve a small technical issue regarding  $\mathbb{Q}$ -factorial terminal singularities which was not fully elucidated in [15]. These are singularities at which uncharged matter localizes. We will remove them by switching on complex structure deformations, as in [16]. This way, we do not have to be concerned about these co-dimensional two effects when we ultimately focus on the main topic of interest in this article, the non-flat torus-fibrations at co-dimension three. Those come naturally about when we relax the constraints on the base space of the F-theory fibration which were imposed in [13, 15]. We find that in the resolved F-Theory four-fold the dimension of the fibre over this point increases, i.e. the fibration becomes non-flat. We study this co-dimension three effect from various angles, and find that in each case we can interpret them as the above mentioned higher order coupling.

Along the way, we determine all the fluxes which are either induced by matter curves [17] and the non-flat fibre. We calculate the second Chern class of the fourfold and look at its implications on the flux quantisation. We give the fluxes which must be turned on to satisfy the quantisation condition and show that this flux forbids string states in four dimensions, coming from M5 branes wrapping the non-flat fibre.

We have organized this paper as follows: in section 2 we review the most relevant geometric aspects of the global  $SU(5) \times U(1)_{PQ}$  as studied in [15]. Then we study the  $\mathbb{Q}$ -factorial terminal singularities which appear in this setting and discuss how to introduce complex structure deformations so that these singularities do not appear. Afterwards we carefully analyse this fibration over a general base without constraints. In section 3, we list all the fluxes coming from the Mordell-Weil group, the matter surfaces, and the non-flat fibres, respectively, and relate them with the quantisation condition and explain why it forbids strings in four-dimensions. In section 4, we take the weak coupling limit of our setting and study the states and their coupling in the IIB picture. As a check, in section 5 we go to the mirror/IIB side to confirm also from this perspective that the non-flat point gives rise to a higher order coupling. Finally, we present our conclusions in section 6.

**Note added.** As we were preparing this paper [18] appeared, which analyzes in detail the physics associated to various non-flat fibrations in codimension two.

---

<sup>2</sup>We would like to thank the referee for emphasizing this point to us.

## 2 The geometric setup

In this section, we review and extend the analysis of the global F-theory realisation of the  $SU(5) \times U(1)$  Peccei-Quinn model [15], cf. [13, 14] for the local description along the GUT-divisor. As a first step, let us first recall the geometric setup presented in section 5 of [15].

To obtain the abelian  $U(1)$  symmetry, we have to start from an elliptic fibration with Mordell-Weil group  $\mathbb{Z}$  [19]. The Weierstraß model realising this symmetry takes the form [20]

$$y^2 = x^3 + \left( C_1 C_3 - B^2 C_0 - \frac{1}{3} C_2^2 \right) x z^4 + \left( C_0 C_3^2 - \frac{1}{3} C_1 C_2 C_3 + \frac{2}{27} C_2^3 - \frac{2}{3} B^2 C_0 C_2 + \frac{1}{4} B^2 C_1^2 \right) z^6, \quad (2.1)$$

with the Mordell-Weil generator, i.e. the second section (besides the zero-section), given by:

$$(x, y, z) = \left( C_3^2 - \frac{2}{3} B^2 C_2^2, -C_3^3 + B^2 C_2 C_3 - \frac{1}{2} B^4 C_1, B \right). \quad (2.2)$$

As described in detail in section 5 of [20], one can resolve the co-dimensional singularities of (2.1) by mapping it into a  $\text{Bl}_{[0,1,0]}\mathbb{P}_{[1,1,2]}$  fibration:

$$B_2 v^2 w + s w^2 + B_1 s w v u + B_0 s^2 w u^2 = C_3 v^3 u + C_2 s v^2 u^2 + C_1 s^2 v u^3 + C_0 s^3 u^4, \quad (2.3)$$

where  $[u, v, w]$  are the homogeneous coordinates of  $\mathbb{P}_{[1,1,2]}$  and  $s$  is the coordinate related to the blow-up of  $\text{Bl}_{[0,1,0]}\mathbb{P}_{[1,1,2]}$ .<sup>3</sup> To obtain in addition to the abelian symmetry the  $SU(5)$ -GUT including the Peccei-Quinn symmetry, meaning that the Higgs up and down multiplets can carry different charges, we have to fix the sections  $B_2, B_1, B_0, C_0, \dots, C_3$ ,<sup>4</sup> in the following way [13–15]:

$$\begin{aligned} B_0 &= -\omega d_3 \alpha = \omega B_{0,1}, \\ B_1 &= -c_2 d_3 = B_{1,0}, \\ B_2 &= \delta = B_{2,0}, \\ C_0 &= \omega^3 \alpha \gamma = \omega^3 C_{0,3}, \\ C_1 &= \omega^2 (d_2 \alpha + c_2 \gamma) = \omega^2 C_{1,2}, \\ C_2 &= \omega c_2 d_2 = \omega C_{2,1}, \\ C_3 &= \omega \beta = \omega C_{3,1}. \end{aligned} \quad (2.4)$$

Here  $\alpha, \beta, \gamma, \delta, d_2, d_3, c_2$  are sections of line bundles of appropriate degree over the base.<sup>5</sup> The  $I_5$ -singular locus, i.e. the GUT-divisor, is at  $\omega = 0$  on the base, as can be readily seen from plugging (2.4) into (2.1) and taking the discriminant.

<sup>3</sup> The toric variety  $\mathbb{P}_{[1,1,2]}$  is directly related to the 6th two-dimensional reflexive polygon, in the standard ordering for such things cf. [11, 12]. Therefore, in the F-theory literature, cf. [21], sometimes (2.3) is known as the “F6-fibration”, a nomenclature we will also use for brevity.

<sup>4</sup>As described in [20], to obtain the coefficients of (2.1) from the coefficients of (2.3), we must do a coordinate shift in  $w$  to get rid of the linear terms, cf. section 4.1.

<sup>5</sup>For base manifolds which are given in terms of toric varieties or embeddings therein, these sections are homogeneous polynomials of certain (multi-)degrees.

Though (2.3) together with (2.4) pose the singular setting of the F-theory model we are interested in, we still have to resolve it to obtain a detailed understanding (via the duality to M-theory) of the physics of this setup. As it turns out [15], (2.3) plus (2.4) does not allow for a resolution of the fibration in a purely torical way. But we can still resolve parts of the hypersurface singularities torically, and only for the final resolution step we have to introduce a complete intersection to represent the smooth Calabi-Yau  $\hat{Y}_4$ . The resolved model is given by the following two hypersurface equations

$$\text{HSE}_1 : \lambda_1 e - \lambda_2 s P_2 = 0, \tag{2.5}$$

$$\text{HSE}_2 : \lambda_2 Q - \lambda_1 u P_1 = 0, \tag{2.6}$$

with the polynomials

$$Q = e_1 s w^2 - e_4^2 e_0 \beta v^3 u + e_4 \delta v^2 w, \tag{2.7}$$

$$P_1 = e_4 e_0 d_2 u v + d_3 w + e_1 e_4 e_0^2 \gamma s u^2, \tag{2.8}$$

$$P_2 = c_2 v + e_0 e_1 \alpha s u. \tag{2.9}$$

The homogeneous coordinates  $[\lambda_1, \lambda_2]$  parameterize the  $\mathbb{P}^1$ , which was added in the final (small) resolution step. To be more precise and for later reference, the two hypersurfaces (2.5) and (2.6) are embedded into the ambient variety with the relations

$u$	$v$	$w$	$s$	$e_0$	$e_1$	$e$	$e_4$	$\lambda_1$	$\lambda_2$	HSE <sub>1</sub>	HSE <sub>2</sub>
1	1	2	0	0	0	0	0	1	0	1	4
0	1	1	1	0	0	0	0	2	0	2	3
$-c_B$	0	0	$[\delta]$	$[\omega]$	0	0	0	$2[\delta] + [\omega] + [\alpha] - c_B$	0	$2[\delta] + [\omega] + [\alpha] - c_B$	$[\delta]$
0	0	-1	0	-1	1	0	0	0	0	0	-1
0	-1	-2	0	-1	0	1	0	-2	0	-1	-4
0	-1	-1	0	-1	0	0	1	-1	0	-1	-2
0	0	0	0	0	0	0	0	1	1	1	1

(2.10)

for the homogeneous coordinates and the Stanley-Reisner ideal:

$$\text{SR-I} = \{u w, u e, u e_4, v s, v e_1, w e_0, s e_0, e_0 e, \lambda_1 \lambda_2, s e, s e_4, w e_4\}. \tag{2.11}$$

Here  $[\cdot]$  means the ‘degree’ of the respective section or polynomial and  $c_B$  is the ‘degree’ of the first Chern class of the base space.

As noted in [15] this complete intersection Calabi-Yau (CICY) still has singularities. A careful analysis of (2.5) and (2.6) yields that there is a remaining singularity at the base loci

$$\alpha = \gamma = 0 \tag{2.12}$$

and fibre coordinates  $w = v = \lambda_1 = 0$ . Indeed, if we assume for the above fibration a two-dimensional base then the so-obtained Calabi-Yau threefold will be  $\mathbb{Q}$ -factorial with terminal singularity points. Such varieties have recently been studied from the F-theory perspective in [16, 22]. There it has been pointed out that such singularities can only be resolved in a discrepant way. Furthermore, upon compactification uncharged hypermultiplets

localise at these singularities which are needed to cancel the six-dimensional gravitational anomaly. It is not too difficult to show that also the fibration at hand has the right amount of uncharged singlets to be anomaly-free. The reader interested in the explicit calculation is pointed to appendix A.

Although these singularities are present in the original setup as presented in [15], we can smooth them away by switching on complex structure deformations [23]. Since the locus (2.12) lies generically away from the GUT-divisor, these deformation do not interfere with the local geometry at  $\omega = 0$  and only alter things away from it. Explicitly, we have to include the higher order terms

$$B_{0,2}, B_{1,1}, C_{0,4}, C_{1,3}, C_{2,2}, \tag{2.13}$$

in (2.4) which will give rise to

$$u^2 w s^2, u v w s, u^4 s^3, u^3 v s^2, u^2 v^2, \tag{2.14}$$

terms in  $Q$ , respectively. The thus obtained smooth geometry is the one we will study throughout the rest of the article.

Most of the details along the GUT-divisor of this  $SU(5) \times U(1)_{PQ}$  fibration have been analysed in [15]. However, due to spectral cover considerations the locus

$$\omega = \alpha = c_2 = 0 \tag{2.15}$$

was excluded. But these loci are always presented if we consider the above setting over a generic three-dimensional base. Therefore, we examine these points very carefully in the following. However, we recall first the most important features of the model. We start with the two **10**-curves:

$$\mathbf{10}_{-2} : d_3 = 0, \quad \mathbf{10}_3 : c_2 = 0, \tag{2.16}$$

and the three **5**-curves:

$$\begin{aligned} \mathbf{5}_{-6} : \delta &= 0, \\ \mathbf{5}_{-1} : \alpha^2 c_2 d_2^2 + \alpha^3 \beta d_3^2 + \alpha^3 d_2 d_3 \delta - 2 \alpha c_2^2 d_2 \gamma - \alpha^2 c_2 d_3 \delta \gamma + c_2^3 \gamma^2 &= 0, \\ \mathbf{5}_4 : \beta d_3 + d_2 \delta &= 0. \end{aligned} \tag{2.17}$$

The Yukawa-points at

$$\begin{aligned} \mathbf{10}_{-2} \bar{\mathbf{5}}_6 \bar{\mathbf{5}}_{-4} : \omega = d_3 = \delta &= 0, \\ \mathbf{10}_{-2} \bar{\mathbf{5}}_1 \bar{\mathbf{5}}_1 : \omega = d_3 = \alpha d_2 - c_2 \gamma, \\ \mathbf{10}_3 \bar{\mathbf{5}}_{-4} \bar{\mathbf{5}}_1 : \omega = c_2 = \beta d_3 + d_2 \delta, \\ \mathbf{10}_{-2} \mathbf{10}_{-2} \mathbf{5}_4 : \omega = d_3 = d_2 &= 0, \\ \mathbf{10}_{-2} \mathbf{10}_3 \mathbf{5}_{-1} : \omega = d_3 = c_2 &= 0, \\ \mathbf{10}_3 \mathbf{10}_3 \mathbf{5}_{-6} : \omega = c_2 = \delta &= 0, \end{aligned} \tag{2.18}$$

and

$$\begin{aligned}
\bar{\mathbf{10}}_{-3} \mathbf{10}_{-2} \mathbf{1}_5 &: \omega = d_3 = c_2 = 0, \\
\bar{\mathbf{5}}_{-4} \mathbf{5}_{-6} \mathbf{1}_{10} &: \omega = \delta = \beta = 0, \\
\bar{\mathbf{5}}_1 \mathbf{5}_{-6} \mathbf{1}_5 &: \omega = \delta = \alpha^2 c_2 d_2^2 + \alpha^3 \beta d_3^2 - 2\alpha c_2^2 d_2 \gamma + c_2^3 \gamma^2 = 0, \\
\bar{\mathbf{5}}_{-4} \mathbf{5}_{-1} \mathbf{1}_5 &: \omega = \beta d_3 + d_2 \delta = \alpha^2 c_2 d_2^2 - 2\alpha c_2^2 d_2 \gamma - \alpha^2 c_2 d_3 \delta \gamma + c_2^3 \gamma^2 = 0,
\end{aligned}
\tag{2.19}$$

have been presented in [15]. Besides these couplings, there is the intersection (2.15) between the  $\mathbf{10}_3$ -curve and the  $\mathbf{5}_{-1}$ -curve for which we cannot write down any gauge invariant three-point interaction. Looking at the second equation in (2.17), we observe that the  $\mathbf{5}_{-1}$ -curve intersects the  $\mathbf{10}_3$ -curve at the points (2.15) three times, i.e. near  $\alpha = c_2 = 0$  the  $\mathbf{5}_{-1}$ -curve takes the form

$$(\alpha - \rho_1 c_2)(\alpha - \rho_2 c_2)(\alpha - \rho_3 c_2) = 0 \tag{2.20}$$

with  $\rho_i$  some constants. This hints already at a four-point coupling  $\mathbf{10}_3 \mathbf{5}_{-1} \mathbf{5}_{-1} \mathbf{5}_{-1}$  but to get a better picture of what really happens at these points, we have to look at the full fourfold geometry, especially the fibre structure. As it turns out, these are points where the dimension of the resolved fibre jumps, i.e. the fibration described by (2.5) and (2.6) over a three-dimensional (or higher dimensional) base is non-flat.<sup>6</sup> The dimensionality jump is due to the vanishing of  $P_2$  at  $\alpha = c_2 = 0$ . We ‘lose’ one of the equations which define the fibral curve of  $E_3$

$$E_3: \quad e = P_2 = \lambda_2 Q - \lambda_1 P_1 = 0. \tag{2.21}$$

A summary of the curves and the coupling points of this setup is depicted in figure 1

### 2.1 Fibre geometry at the non-flat points

Let us now present the details of the fibre above the non-flat points. At  $\omega = \alpha = c_2 = 0$ , the  $\mathbb{P}^1$ -curves of  $E_1$ ,  $E_3$  and  $E_4$  split (or extend in dimension) in the following way

$$\begin{aligned}
\mathbb{P}_{E_1}^1 &\rightarrow \{\mathbb{P}_{\text{nf}_1}^1 : e_1 = e_4 = \lambda_1 = 0, \mathbb{P}_{\text{nf}_2}^1 : e_1 = u e_0 e_4 \beta - w \delta = \lambda_1 = 0, \\
&\quad \mathbb{P}_{\text{nf}_3}^1 : e_1 = e = \lambda_2 (u e_0 e_4^2 \beta - w e_4 \delta) + \lambda_1 (u^2 e_0 e_4 d_2 + u w d_3) = 0\}, \\
\mathbb{P}_{E_3}^1 &\rightarrow \{\mathcal{FS} : e = \lambda_2 (v^3 e_4^2 \beta - v^2 w e_4 \delta - w^2 e_1) + \lambda_1 (e_1 e_4 \gamma + v e_4 d_2 + w d_3) = 0\}, \\
\mathbb{P}_{E_4}^1 &\rightarrow \{\mathbb{P}_{\text{nf}_1}^1 : e_1 = e_4 = \lambda_1, \mathbb{P}_{\text{nf}_4}^1 : e = e_4 = e_1 \lambda_2 - \lambda_1 d_3\},
\end{aligned}
\tag{2.22}$$

whereas the fibres of  $E_0$  and  $E_2$  remain intact.<sup>7</sup> The Cartan charges of the above  $\mathbb{P}^1$ 's are:

$$\begin{aligned}
\mathbb{P}_{\text{nf}_1}^1 &: (-1, 0, 1, -1)_{-3} \subset \bar{\mathbf{10}}_{-3}, \\
\mathbb{P}_{\text{nf}_2}^1 &: (-1, 0, 1, 0)_3 \subset \mathbf{10}_3, \\
\mathbb{P}_{\text{nf}_3}^1 &: (0, 1, -2, 1)_0 \subset \text{roots}, \\
\mathbb{P}_{\text{nf}_4}^1 &: (1, 0, 0, -1)_3 \subset \mathbf{10}_3.
\end{aligned}
\tag{2.23}$$

<sup>6</sup>This does not imply that the dimension of the fourfold changes nor that it is singular at these points.

<sup>7</sup>We should note here that for a different phase of the Coulomb branch, i.e. for another SR-ideal, the splitting can be different.

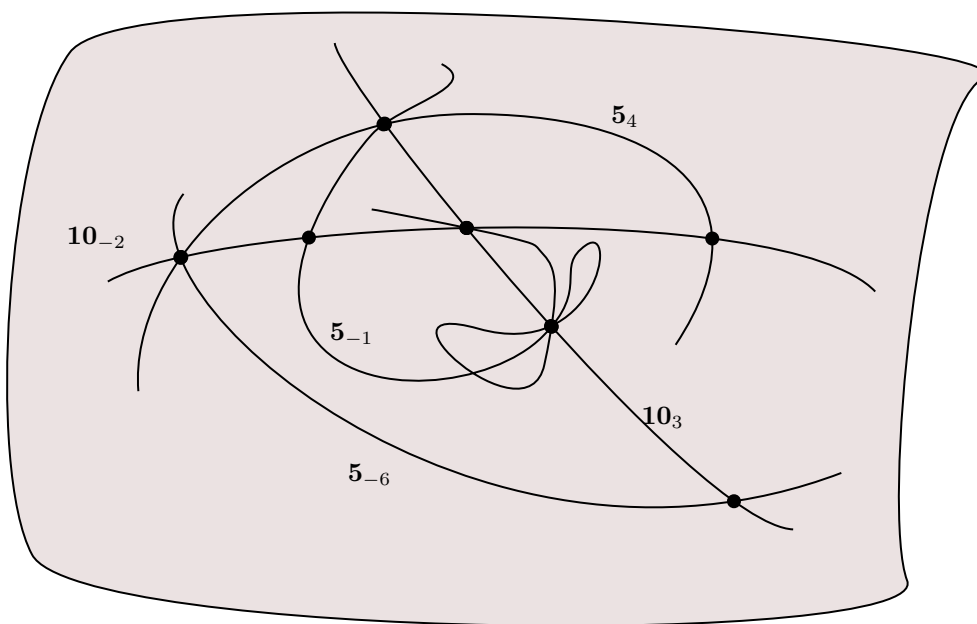


**Figure 1.** A sketch of the matter curves and Yukawa points within the SU(5) GUT divisor  $\{\omega = 0\}$ . The seven bold dots indicate the six Yukawa points of (2.18) plus the triple intersection of the  $5_{-1}$ -curve with the  $10_3$ -curve.

To see that the fibre surface  $\mathcal{FS}$  at the non-flat points are del Pezzo four surfaces at a special complex structure sublocus, we give the reduced ambient space:

$v$	$e_1$	$w$	$e_4$	$\lambda_1$	$\lambda_2$	$\sum$	$\text{HSE}_2^{\text{red}}$
1	1	1	0	2	0	5	3
0	0	1	1	1	0	3	2
0	0	0	0	1	1	2	1

(2.24)

into which

$$\text{HSE}_2^{\text{red}} : \lambda_2 (v^3 e_4^2 \beta - v^2 w e_4 \delta - w^2 e_1) + \lambda_1 (e_1 e_4 \gamma + v e_4 d_2 + w d_3) = 0 \quad (2.25)$$

is embedded. The polynomials  $\beta, \delta, \gamma, d_2, d_3$  from beforehand are now effectively coefficients. The toric space (2.24) is a  $\mathbb{P}^1$ -fibration over the Hirzebruch surface  $\mathbb{F}_1 \cong d\mathbb{P}_1$  and (2.25) defines a section of this fibration. Since the section degenerates over the points

$$v^3 e_4^2 \beta - v^2 w e_4 \delta - w^2 e_1 = e_1 e_4 \gamma + v e_4 d_2 + w d_3 = 0, \quad (2.26)$$

the del Pezzo one surface is blown up at three points. These three points lie along a line. Therefore, the fibre-surface  $\mathcal{FS}$  is not a generic del Pezzo four surface but a degenerate  $d\mathbb{P}_4$ .  $\mathcal{FS}$  contains several rational curves: the generic fibre and the two special sections of  $\mathbb{F}_1$ ; from the blow-ups of the Hirzebruch surface, we have the line going through the

blown-up points, the exceptional  $\mathbb{P}^1$ 's, and the proper transforms of the fibres at these points. The Cartan charges of the rational lines are:

$$\begin{aligned}
 \mathbb{P}_{\text{fibre}}^1 &\cong \mathbb{P}_{\text{nf}_3}^1 \rightarrow (0, 1, -2, 1)_0, \\
 \mathbb{P}_{\text{sec}_1}^1 &= \{e = w = \text{HSE}_2^{\text{red}} = 0\} \rightarrow (1, 1, -2, 0)_3, \\
 \mathbb{P}_{\text{sec}_2}^1 &\cong \mathbb{P}_{\text{nf}_4}^1 \rightarrow (1, 0, 0, -1)_3, \\
 \mathbb{P}_{\text{line}}^1 &= \{e = \lambda_2 = e_1 e_4 \gamma + v e_4 d_2 + w d_3 = 0\} \rightarrow (1, -2, 1, 0)_0, \\
 \mathbb{P}_{\text{bu}_i}^1 &= \{e = 0 \wedge (2.26)\} \rightarrow (0, 1, -1, 0)_1, \\
 \mathbb{P}_{\text{p.t.-fib}_i}^1 &\cong \mathbb{P}_{\text{fibre}}^1 - \mathbb{P}_{\text{bu}_i}^1 \rightarrow (0, 0, -1, 1)_{-1}.
 \end{aligned}
 \tag{2.27}$$

Regarding  $\mathbb{P}_{\text{line}}^1$ , we should note that prior to the blow-ups it was equivalent to  $\mathbb{P}_{\text{sec}_1}^1$ , i.e.  $\mathbb{P}_{\text{line}}^1$  is the proper transform of  $\text{sec}_1$  going through the three points which are blown-up. Hence, there are two special points for the complex structure deformation of  $\mathbb{P}_{\text{sec}_1}^1$ ; one where it splits into

$$\mathbb{P}_{\text{sec}_1}^1 \rightarrow \mathbb{P}_{\text{line}}^1 + \sum_{i=1}^3 \mathbb{P}_{\text{bu}_i}^1$$

and the one, which existed already in  $\mathbb{F}_1$ , where it becomes reducible to

$$\mathbb{P}_{\text{sec}_1}^1 \rightarrow \mathbb{P}_{\text{sec}_2}^1 + \mathbb{P}_{\text{fibre}}^1.$$

With these details at hand, we can describe the three-cycle which fuses three  $\bar{\mathbf{5}}_1$  states into a  $\mathbf{10}_3$  state:

$$\begin{aligned}
 (0, 1, -1, 0)_1 + (1, -1, 0, 0)_1 + (-1, 0, 0, 0)_1 &\rightarrow (3 \times (0, 1, -1, 0)_1 + (1, -2, 1, 0)_0) \\
 &+ (1, -2, 1, 0)_0 + (-2, 1, 0, 0)_0 \rightarrow (1, 1, -2, 0)_3 + (1, -2, 1, 0)_0 \\
 &+ (-2, 1, 0, 0)_0 \rightarrow (1, 0, 0, -1)_3 + (0, 1, -2, 1)_0 + (1, -2, 1, 0)_0 \\
 &+ (-2, 1, 0, 0)_0 \rightarrow (0, 0, -1, 0)_3.
 \end{aligned}
 \tag{2.28}$$

In figure 2, we sketched  $\mathcal{FS}$  to better understand the interplay of the rational curves.

### 3 Fluxes

Now that we have gained insight on the geometry of our model, we can turn to the F-theory four-form flux of our setup. It has to fulfil the flux quantisation condition [24, 25]:

$$G_4 + \frac{1}{2}c_2(\hat{Y}_4) \in H^4(\hat{Y}_4, \mathbb{Z}),
 \tag{3.1}$$

with  $\hat{Y}_4$  the resolved Calabi-Yau four-fold. To see whether (3.1) forces us to switch on half-integer fluxes, we are analysing in the following the Chern class of our four-fold (2.5)–(2.11). The main goal of this study is to prove that the restriction of  $G_4$  to the non-flat fiber gives rise to a non-trivial homology class. This fact provides a nice simplification of the physics of the system, since it immediately implies that the M5 brane wrapping this

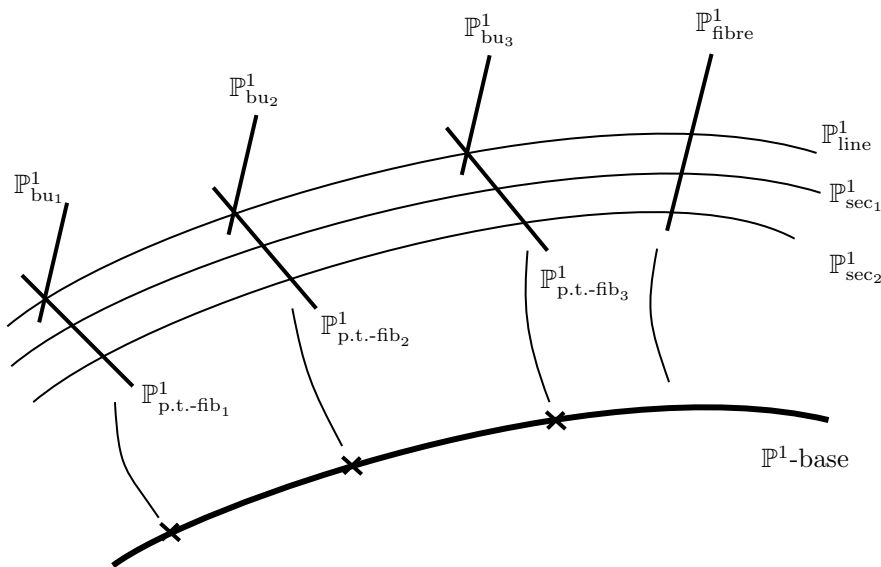


**Figure 2.** Schematic drawing of the fibration structure of fibre surface  $\mathcal{FS}$ .

divisor is inconsistent [25]. Accordingly, the four dimensional light strings this wrapped M5 would give rise to in four dimensions are absent.<sup>8</sup>

Let us also mention that non-trivial flux will potentially induce chirality, and thus anomaly cancellation is a worry. Our goal in this note is to clarify the dynamics arising from the non-flat (codimension-three) point, while anomaly cancellation is a more global phenomenon arising from matter curves, at codimension two. Therefore, we expect our considerations to hold regardless of whether anomalies are ultimately canceled in any specific model, as long as the local behavior is as in our example. Even if not immediately relevant to us, the details of anomaly cancellation could be interesting. For example if there were underlying algebraic relations like the one observed in [27]. We will leave such an analysis for future work.

### 3.1 The second Chern class

Let us start by giving the second Chern class of an elliptically fibred fourfold  $\hat{Y}_4$  where the torus fibre is F6 (in the nomenclature of footnote 3). For such manifolds, where we did not impose an SU(5) singularity yet, the second Chern class reads<sup>9</sup>

$$c_2(\hat{Y}_4) = (c_2(B_3) - c_1(B_3)^2) + 6 c_1(B_3) (S+U+c_1(B_3)-[\delta]) - [\delta] (S-U-c_1(B_3)-[\delta]). \quad (3.2)$$

<sup>8</sup>Note that even if the flux was trivial, this would not necessarily imply that the strings are light: they could still obtain a mass from periods of  $C_3$ , as conjectured in [26] in a closely related case. But the existence of the flux makes the point moot.

<sup>9</sup>Here and in the following, we denote by capital letters the divisor class corresponding to the homogeneous coordinate given in terms of lower case letters, i.e.  $U$  is the divisor class of the locus  $\{u = 0\}$ . In the case of polynomials we use square brackets, i.e.  $[c_2]$  denotes the divisor class with representative  $\{c_2 = 0\}$ .

Hence, depending on the degree of  $[\delta]$ , when considering such an F-theory compactification one might be forced to switch on flux even though no non-abelian gauge groups are present yet. Note that this is different from the  $U(1)_X$  case [28, 29].

### 3.2 U(1)- and matter surface fluxes

Before coming to the second Chern class of the model including the  $SU(5)$ , we write down the different fluxes which we can construct from the Mordell-Weil generator and the matter surfaces. This helps us in the next section to give the second Chern class in a concise way.

From the section  $S$  we obtain via the Shioda map [30–32] the following expression for the  $U(1)$ -flux:

$$G_4^{U(1)}(\mathcal{F}) = \mathcal{F} (5 (S - U - [\delta] - c_1(B_3)) + 4 E_1 + 3 \Lambda_2 + 2 (E - \Lambda_2) + E_4) \quad (3.3)$$

with  $\mathcal{F} \in \pi^* H^{1,1}(B_3, \mathbb{Z})$ . To construct from the matter surfaces gauge invariant fluxes, we follow a similar strategy to the one presented in [17]. That way we obtain the following fluxes:

$$\begin{aligned} G_4(\mathbf{10}_{-2}) &= 5 (E_1 - \Lambda_1) E_4 - (2 c_1(B_3) - ([\delta] + [\alpha] + [\omega])) \\ &\quad \times (2 E_1 - \Lambda_2 + (E - \Lambda_2) + 3 E_4), \\ G_4(\mathbf{10}_3) &= 5 \Lambda_1 E_4 - ([\delta] + [\alpha] + [\omega] - c_1(B_3))(3 E_1 + \Lambda_2 - (E - \Lambda_2) + 2 E_4), \\ G_4(\mathbf{5}_{-6}) &= 5 E_1 U - [\delta] (4 E_1 + 3 \Lambda_2 + 2 (E - \Lambda_2) + E_4), \\ G_4(\mathbf{5}_{-1}) &= ([P_1] - \Lambda_2)([P_2] - \Lambda_1) + S [P_1] - (4 c_1(B_3) - 2 [\delta] - 3 [\omega] - [\alpha]) \\ &\quad \times (-E_1 - 2 \Lambda_2 + 2 (E - \Lambda_2) + E_4), \\ G_4(\mathbf{5}_4) &= 5 (E_1 ([P_1] - \Lambda_2 - E_4) + \Lambda_1 E_4) - (3 c_1(B_3) - ([\alpha] + 2 [\omega])) \\ &\quad \times (E_1 - 3 \Lambda_2 - 2 (E - \Lambda_2) - E_4). \end{aligned} \quad (3.4)$$

### 3.3 Second Chern class of the $SU(5) \times U(1)_{PQ}$ fourfold

With all these expressions at hand, we can now finally give the second Chern class of the fourfold  $\hat{Y}_4$  under consideration:

$$\begin{aligned} c_2(\hat{Y}_4) &= (c_2(B_3) - c_1(B_3)^2) + 6 c_1(B_3) (S + U + c_1(B_3) - [\delta]) \\ &\quad - G_4^{U(1)}(\omega) - G_4(\mathbf{10}_{-2}) - G_4(\mathbf{5}_4) - G_4^{\text{mf}} + \text{even terms} \\ &= G_4^{U(1)}(\omega) + G_4(\mathbf{10}_{-2}) + G_4(\mathbf{5}_4) + G_4^{\text{mf}} + \text{even terms}. \end{aligned} \quad (3.5)$$

Here  $G_4^{\text{mf}}$  is the flux corresponding to the four cycle  $\mathcal{FS}$ :

$$G_4^{\text{mf}} = [c_2] (E - \Lambda_2 - E_1) + E_1 (\Lambda_1 - S). \quad (3.6)$$

The main properties of the  $G_4^{\text{mf}}$  flux are that it does not break the  $SU(5)$  gauge symmetry and it localises at the non-flat points. To see the second, we can integrate  $G_4^{\text{mf}}$  over all algebraic two-cycles in  $\hat{Y}_4$  which are accessible to us, i.e.

$$\int_{\hat{Y}_4} G_4^{\text{mf}} \mathcal{C}_i = 0 \quad (3.7)$$

with

$$\mathcal{C}_i = \{\Gamma \tilde{\Gamma}, U \Gamma, S \Gamma, E_1 \Gamma, \Lambda_2 \Gamma, E \Gamma, E_4 \Gamma, E_4 \Lambda_2, U E_1\}_i, \quad i = 1, \dots, 9 \quad (3.8)$$

and

$$\int_{\hat{Y}_4} G_4^{\text{nf}} \mathcal{C}_{10} \neq 0, \quad \int_{\mathcal{FS}} G_4^{\text{nf}} = \int_{\hat{Y}_4} G_4^{\text{nf}} \mathcal{C}_{11} \neq 0 \quad (3.9)$$

where  $\mathcal{C}_{10} = E_1 E_4$  and  $\mathcal{C}_{11}$  is the four-cycle of the non-flat fibre. In equation (3.8)  $\Gamma$  and  $\tilde{\Gamma}$  are place holders for all possible divisor classes pulled back from the base  $B_3$ .

Before we can make our main point of this section, we should first notice that all odd fluxes besides  $G_4^{\text{nf}}$  appearing in (3.5) do not localise at the non-flat points, i.e.

$$\int_{\mathcal{FS}} c_2(\hat{Y}_4)|_{\mathcal{FS}} = \int_{\mathcal{FS}} G_4^{\text{nf}}. \quad (3.10)$$

Therefore, we conclude that by (3.1) there must be a non-trivial  $G_4$  flux on  $\hat{Y}_4$ , whose restriction to  $\mathcal{FS}$  cancels this contribution.

## 4 The weak coupling limit and the IIB picture

As we will argue, the F-theory model of interest to us can be taken to weak coupling without breaking any of the GUT symmetries, and without encountering any special behavior along the way. Since we are interested in computing a superpotential coupling, which is a holomorphic quantity, we expect that the result of computing such quantities at weak coupling remains valid all through moduli space.

### 4.1 Weak coupling limit

We recall from section 2 that the generic elliptic fibre with one free Mordell-Weil generator, i.e.

$$c_0 u^4 + c_1 u^3 v + c_2 u^2 v^2 + c_3 u v^3 + b_0 u^2 w + b_1 u v w + b_2 v^2 w + w^2 = 0, \quad (4.1)$$

can be brought via a birational transformation into Tate form

$$y^2 + a_1 x y z + a_3 y z^3 = x^3 + a_2 x^2 z^2 + a_4 x z^4 + a_6 z^6, \quad (4.2)$$

with

$$\begin{aligned} a_1 &= b_1 \\ a_2 &= -(b_2 c_1 + b_0 c_3) \\ a_3 &= -(b_0 b_2 + c_2) \\ a_4 &= (b_2^2 c_0 + b_0 b_2 c_2 + c_1 c_3) \\ a_6 &= -(b_2^2 c_0 c_2 - b_1 b_2 c_0 c_3 + b_0 b_2 c_1 c_3 + c_0 c_3^2). \end{aligned} \quad (4.3)$$

In analogy to [33], we define

$$\begin{aligned} \mathbf{b}_2 &= a_1^2 + 4 a_2 \\ \mathbf{b}_4 &= a_1 a_3 + 2 a_2^2 \\ \mathbf{b}_6 &= a_3^2 + 4 a_6. \end{aligned} \tag{4.4}$$

To take the weak coupling limit, we proceed along the lines of Sen's original work [34] and require  $\mathbf{b}_2$ ,  $\mathbf{b}_4$ , and  $\mathbf{b}_6$  to scale (at leading order) like  $\epsilon^0$ ,  $\epsilon^1$ , and  $\epsilon^2$ , respectively, as we take the limit  $\epsilon \rightarrow 0$ . One way to obtain that behaviour is to take

$$c_i \rightarrow \epsilon c_i, \tag{4.5}$$

in (4.4). Collecting the constant term in  $\mathbf{b}_2 = R + O(\epsilon)$  the linear term in  $\mathbf{b}_4 = S\epsilon + O(\epsilon^2)$  and the quadratic term in  $\mathbf{b}_6 = T\epsilon^2 + O(\epsilon^3)$  we can write the discriminant in the weak coupling limit as

$$\Delta = \frac{1}{4} R^2 (-RT + S^2) \epsilon^2 + O(\epsilon^3) =: \epsilon^2 R^2 \Delta_{w.c.} + O(\epsilon^3). \tag{4.6}$$

Plugging (4.3) into  $\Delta_{w.c.}$ , we obtain the rather lengthy polynomial

$$\begin{aligned} \Delta_{w.c.} \sim b_2 & \left( b_2^3 c_0^2 - b_1 b_2^2 c_0 c_1 + b_0 b_2^2 c_1^2 - 2 b_0 b_2^2 c_0 c_2 + b_1^2 b_2 c_0 c_2 \right. \\ & - b_0 b_1 b_2 c_1 c_2 + b_0^2 b_2 c_2^2 + 3 b_0 b_1 b_2 c_0 c_3 - 2 b_0^2 b_2 c_1 c_3 - b_1^3 c_0 c_3 \\ & \left. + b_0 b_1^2 c_1 c_3 - b_0^2 b_1 c_2 c_3 + b_0^3 c_3^2 \right). \end{aligned} \tag{4.7}$$

This is the IIB D-brane locus (without the orientifold plane) for the generic F6-fibration if we take the weak coupling limit as in (4.5). The corresponding Calabi-Yau threefold is given by following double cover of  $B_3$ :

$$\xi^2 - R = 0, \tag{4.8}$$

where the vanishing set  $\{R = 0\}$  defines the orientifold plane and the orientifold action is naturally induced by

$$\xi \longleftrightarrow -\xi. \tag{4.9}$$

Now we restrict the section  $b_i$  and  $c_i$  to the case we are interested in, i.e.  $SU(5) \times U(1)_{PQ}$  [15]:

$$\begin{aligned} b_0 &= -\omega d_3 \alpha + b_{0,2} \omega^2, & b_1 &= -c_2 d_3 + b_{1,1} \omega, & b_2 &= \delta, \\ c_0 &= -\omega^3 \alpha \gamma, & c_1 &= -\omega^2 (d_2 \alpha + c_2 \gamma), & c_2 &= -\omega c_2 d_2, \\ c_3 &= -\omega \beta. \end{aligned} \tag{4.10}$$

where, for convenience, we switch on only one complex structure deformation compared with [15], cf. equation (2.13). Thus, we obtain

$$\xi^2 + c_2^2 d_3^2 + \omega (b_{1,1}^2 \omega - 4 b_{0,2} \omega \delta + 4 \alpha \delta d_3 - 2 b_{1,1} c_2 d_3) = 0 \tag{4.11}$$

for the hypersurface of the Calabi-Yau threefold. We do not show the rather lengthy expression for  $\Delta_{w.c.}$  because it will turn out that in suitable coordinates the polynomial

factorizes and the loci of the brane-image brane pair become evident. We work now close to the singular point<sup>10</sup>

$$\xi = \omega = c_2 = \alpha = 0, \tag{4.12}$$

where we expect the higher order coupling to arise. In particular, we assume that all  $d_3$  and  $\delta$  are non-vanishing close to the points of interest. We define now

$$(u, w, \sigma) := (c_2 d_3, b_{1,1}^2 \omega - 4 b_{0,2} \omega \delta + 4 \alpha \delta d_3 - 2 b_{1,1} c_2 d_3, \omega), \tag{4.13}$$

such that the ordinary double point singularity, or conifold, takes the form

$$\xi^2 = u^2 + \sigma w. \tag{4.14}$$

We can represent this conifold also in a toric way by introducing the homogeneous coordinate  $\alpha_i, \beta_i$  with  $i = 1, 2$  and scaling relation:

$$\frac{\alpha_1 \mid \alpha_2 \mid \beta_1 \mid \beta_2}{1 \mid 1 \mid -1 \mid -1} \tag{4.15}$$

where

$$|\alpha_1|^2 + |\alpha_2|^2 - |\beta_1|^2 - |\beta_2|^2 = 0. \tag{4.16}$$

The affine coordinates from above are expressed in terms of homogeneous ones as

$$(\xi, u, \sigma, w) = \left( \frac{1}{2} (\alpha_1 \beta_2 - \alpha_2 \beta_1), \frac{1}{2} (\alpha_1 \beta_2 + \alpha_2 \beta_1), -\alpha_1 \beta_1, \alpha_2 \beta_2 \right). \tag{4.17}$$

Furthermore, the orientifold involution (4.9) acts now via

$$\alpha_i \longleftrightarrow \beta_i. \tag{4.18}$$

Using these two coordinate changes, we can rewrite the D-brane locus close to the point of interest as follows:

$$\begin{aligned} \Delta_{w.c.} \sim & \alpha_1^5 \beta_1^5 \left( (-2 b_{1,1}^2 \delta^2 \gamma + 8 b_{0,2} \delta^3 \gamma + b_{1,1}^3 \delta d_2 - 4 b_{0,2} b_{1,1} \delta^2 d_2 - b_{1,1}^3 \beta d_3) \alpha_1^3 \right. \\ & + (-2 b_{1,1}^2 \delta d_2 + 8 b_{0,2} \delta^2 d_2 + 6 b_{1,1}^2 \beta d_3) \alpha_1^2 \alpha_2 \\ & + (8 \delta^2 \gamma - 4 b_{1,1} \delta d_2 - 12 b_{1,1} \beta d_3) \alpha_1 \alpha_2^2 + (8 \delta d_2 + 8 \beta d_3) \alpha_2^3 \Big) \\ & \times \left( (-2 b_{1,1}^2 \delta^2 \gamma + 8 b_{0,2} \delta^3 \gamma + b_{1,1}^3 \delta d_2 - 4 b_{0,2} b_{1,1} \delta^2 d_2 - b_{1,1}^3 \beta d_3) \beta_1^3 \right. \\ & + (-2 b_{1,1}^2 \delta d_2 + 8 b_{0,2} \delta^2 d_2 + 6 b_{1,1}^2 \beta d_3) \beta_1^2 \beta_2 \\ & + (8 \delta^2 \gamma - 4 b_{1,1} \delta d_2 - 12 b_{1,1} \beta d_3) \beta_1 \beta_2^2 + (8 \delta d_2 + 8 \beta d_3) \beta_2^3 \Big). \end{aligned} \tag{4.19}$$

---

<sup>10</sup>The hypersurface (4.11) has obviously more singularities than the one at (4.12). There, is for instance, a co-dimension two singularity along  $\xi = \omega = d_3 = 0$ . However, we will ignore this singularity because first of all we are only interested in the vicinity of (4.12) and secondly we could either resolve it or chose a fibration where  $d_3$  is constant. All the other co-dimension three singularities can be treated like [26], cf. below.

This makes it obvious that the flavor brane/image brane pair are respectively located at

$$P_1 = \eta_0 \alpha_1^3 + \eta_1 \alpha_1^2 \alpha_2 + \eta_2 \alpha_1 \alpha_2^2 + \eta_3 \alpha_2^3 = 0 \tag{4.20}$$

$$P_2 = \eta_0 \beta_1^3 + \eta_1 \beta_1^2 \beta_2 + \eta_2 \beta_1 \beta_2^2 + \eta_3 \beta_2^3 = 0, \tag{4.21}$$

whereas the GUT stack and image-stack are at  $\alpha_1 = 0$  and  $\beta_1 = 0$ , respectively. Locally the  $\eta_i$ 's are invertible and we treat them as if they were non-zero complex numbers. Under this assumption, we can further factorise the flavour branes to

$$P_1 = \prod_{i=1}^3 (A^i \alpha_1 + B^i \alpha_2), \tag{4.22}$$

$$P_2 = \prod_{i=1}^3 (A^i \beta_1 + B^i \beta_2). \tag{4.23}$$

This implies that close to the point of interest there are three incoming flavor branes  $A^i \alpha_1 + B^i \alpha_2$  each with their respective mirror  $A^i \beta_1 + B^i \beta_2$ .

## 4.2 Ext groups and quiver theory

In order to construct the resulting gauge theory, we need to specify all branes participating at the point of interest. Following [26], we employ the method of non-commutative crepant resolutions [35]. This entails describing branes as elements of the derived category of quasi-coherent sheaves on say  $Y_+$ . Open string states between these are expressed in terms of morphisms between such objects, which in turn are elements of so called Ext groups. (For a review of the relevant background material aimed at physicists, see [36].) We will first briefly review the general form of the construction for the conifold in section 4.2.1, and will then apply this construction to our non-flat point in section 4.2.2.

### 4.2.1 Non-commutative crepant resolution of the conifold

Consider again the singular conifold, described by

$$\text{Spec } (\mathbb{C}[\xi, u, w, \sigma] / \langle \xi^2 - u^2 - \sigma w \rangle). \tag{4.24}$$

This, as we saw above, is a toric variety

$$\begin{array}{c|c|c|c} \alpha_1 & \alpha_2 & \beta_1 & \beta_2 \\ \hline 1 & 1 & -1 & -1 \end{array}. \tag{4.25}$$

The conifold has two small crepant resolutions which correspond in toric language to different subdivisions of its fan. These are also toric varieties with homogeneous coordinates  $\alpha_1, \dots, \beta_2$  subject to the constraint

$$|\alpha_1|^2 + |\alpha_2|^2 - |\beta_1|^2 - |\beta_2|^2 = t. \tag{4.26}$$

The two small resolutions are distinguished by the sign of  $t$ , and we denote them as  $Y_{\pm}$  respectively. Applying the orientifold involution (4.18) to (4.26), we see that  $t \leftrightarrow -t$ , that is to say the two resolutions  $Y_{\pm}$  are exchanged. This means that the resolution mode corresponding to the  $\mathbb{P}^1$  is projected out.

It is, however, possible to describe D-branes on the singular space directly using its non-commutative crepant resolution [35]. By this we mean a non-commutative ring  $A$

$$A = \text{End}(M \oplus R), \tag{4.27}$$

where  $R = \mathbb{C}[\xi, u, w, \sigma]/\langle \xi^2 - u^2 - \sigma w \rangle$  and  $M$  is

$$M = \text{coker}(\psi : R^2 \rightarrow R^2). \tag{4.28}$$

Here the map  $\psi$  is given by

$$\psi = \begin{pmatrix} \xi + u & \sigma \\ w & \xi - u \end{pmatrix}. \tag{4.29}$$

Notice that one could also take

$$M = \text{coker}(\phi : R^2 \rightarrow R^2), \tag{4.30}$$

with

$$\phi = \begin{pmatrix} \xi - u & -\sigma \\ -w & \xi + u \end{pmatrix}. \tag{4.31}$$

Observe that

$$\phi\psi = \psi\phi = (\xi^2 - u^2 - \sigma w) \begin{pmatrix} 1 & 0 \\ 0 & 1 \end{pmatrix}. \tag{4.32}$$

We do not want to delve into the details but simply state that  $A$  is derived equivalent to  $Y_{\pm}$ . More concretely there is a correspondence

$$D^b(\text{mod}(A)) \cong D^b(\text{QCoh}(Y_{\pm})), \tag{4.33}$$

cf. Theorem 5.1 in [35]. As is well established [36], one can view objects of  $D^b(\text{QCoh}(Y_{\pm}))$  as D-branes in the B-model and morphisms between them correspond to open strings states.

Using the dictionary laid out in [26], we will map certain (complexes of)  $A$ -modules to D-branes of interest. In order describe these effectively note that

$$A = \text{End}(M \oplus R) = \text{End}(R, R) \oplus \text{End}(A, A) \oplus \text{End}(A, M) \oplus \text{End}(M, A). \tag{4.34}$$

As a quiver we can represent  $A$  as

$$e_0 \curvearrowright R \begin{matrix} \xrightarrow{\alpha_{1,2}} \\ \xleftarrow{\beta_{1,2}} \end{matrix} M \curvearrowright e_1 \tag{4.35}$$

Here

$$\text{End}(R, R) = \langle e_0 \rangle \cong R \tag{4.36}$$

$$\text{End}(R, R) = \langle e_1 \rangle \cong R \tag{4.37}$$

$$\text{End}(R, M) = \langle \alpha_1, \alpha_2 \rangle \tag{4.38}$$

$$\text{End}(M, R) = \langle \beta_1, \beta_2 \rangle, \tag{4.39}$$

as  $R$ -vector spaces. In particular,  $e_i$  are idempotents.

Any module of  $A$  can be encoded as a quiver representation. As laid out in [26], the basic representations from which one builds D7-branes are:

$$P_0 = e_0 A, \tag{4.40}$$

$$P_1 = e_1 A. \tag{4.41}$$

These are linear combinations of paths ending at the left and right node of the quiver (4.35), respectively. Clearly morphisms from  $P_0$  to  $P_1$  are generated by  $\alpha_{1,2}$  and from  $P_1$  to  $P_0$  by  $\beta_{1,2}$ . Together with the assignment

$$P_0 \mapsto \mathcal{O} \tag{4.42}$$

$$P_1 \mapsto \mathcal{O}(1), \tag{4.43}$$

where  $\mathcal{O}$  is the structure sheaf of the resolved conifold, we obtain for instance

$$\left( P_0 \xrightarrow{\alpha_1} P_1 \right) \mapsto \left( \mathcal{O} \xrightarrow{\alpha_1} \mathcal{O}(1) \right). \tag{4.44}$$

Here the map  $\alpha_1$  between the sheaves is nothing but the fiberwise multiplication by the homogeneous coordinate. The power of this approach is that computing Ext-groups between complexes of sheaves is easier in the setting of quiver representations. Since all relevant computations were already carried out in [26], we will not demonstrate them but only list the results in the following.

Fractional branes given by D1-branes wrapping the resolution divisor are given by

$$S_0 = \mathbb{C}\langle e_0 \rangle \tag{4.45}$$

$$S_1 = \mathbb{C}\langle e_1 \rangle. \tag{4.46}$$

In terms of diagrams

$$e_0 \curvearrowright \mathbb{C} \begin{array}{c} \xrightarrow{0} \\ \xleftarrow{0} \end{array} \{0\} \curvearrowright 0$$

and

$$0 \curvearrowright \{0\} \begin{array}{c} \xrightarrow{0} \\ \xleftarrow{0} \end{array} \mathbb{C} \curvearrowright e_1$$

We will later indicate the what the objects  $S_0, S_1$  look like in  $D^b(Y_+)$ . It is, however, convenient to define  $I_0 = S_0[-1]$  and  $I_1 = S_1[-1]$ . Then we can represent the resolved conifold by

$$e_0 \curvearrowright I_0 \begin{array}{c} \xrightarrow{\alpha_i} \\ \xleftarrow{\beta_i} \end{array} I_1 \curvearrowright e_1 \tag{4.47}$$

This follows from the fact that the moduli space of representations of dimension  $(1, 1)$  is exactly the resolved conifold, see [26] section 3.2.1.

The brane/image brane pairs appearing in this paper are

$$F_0^i = \mathcal{O} \xrightarrow{A^i\alpha_1+B^i\alpha_2} \mathcal{O}(1) \in \text{Obj}(\mathcal{D}^b(Y_+)) \quad (4.48)$$

$$F_1^i = \mathcal{O} \xrightarrow{A^i\beta_1+B^i\beta_2} \mathcal{O}(-1) \in \text{Obj}(\mathcal{D}^b(Y_+)). \quad (4.49)$$

These correspond to D7 branes located at the **5** curve. To see this apply the cokernel to the relevant maps, which is commonly referred to as Tachyon condensation. Moreover there is one pair of objects corresponding to D7 branes located at the **10** curve

$$G_0 = \mathcal{O} \xrightarrow{\alpha_1} \mathcal{O}(1) \in \text{Obj}(\mathcal{D}^b(Y_+)) \quad (4.50)$$

$$G_1 = \mathcal{O} \xrightarrow{\beta_1} \mathcal{O}(-1) \in \text{Obj}(\mathcal{D}^b(Y_+)). \quad (4.51)$$

We also have fractional branes D(-1) instantons described by objects  $I_0 = S_0[-1]$  and  $I_1 = S_1[-1]$  where

$$S_0 = \mathcal{O}(2) \xrightarrow{\begin{pmatrix} \beta_2 \\ -\beta_1 \end{pmatrix}} \mathcal{O}(1)^{\oplus 2} \xrightarrow{(\beta_1, \beta_2)} \mathcal{O} \in \text{Obj}(\mathcal{D}^b(Y_+)) \quad (4.52)$$

$$S_1 = \mathcal{O}(1) \xrightarrow{\begin{pmatrix} -\beta_2 \\ \beta_1 \end{pmatrix}} \mathcal{O}^{\oplus 2} \xrightarrow{(\beta_1, \beta_2)} \mathcal{O}(-1) \longrightarrow 0 \quad (4.53)$$

For more details on this see appendix A of [26].

We now study the open string states between these branes by computing certain Ext groups between elements of  $\mathcal{D}^b(Y_+)$ , where  $Y_+$  is one of the crepant small resolutions of the conifold. To this end consider the pair

$$F_0^i = \mathcal{O} \xrightarrow{A^i\alpha_1+B^i\alpha_2} \mathcal{O}(1) \in \text{Obj}(\mathcal{D}^b(Y_+)). \quad (4.54)$$

$$F_1^i = \mathcal{O} \xrightarrow{A^i\beta_1+B^i\beta_2} \mathcal{O}(-1) \in \text{Obj}(\mathcal{D}^b(Y_+)). \quad (4.55)$$

The groups  $\text{Ext}^i(F_0, F_1)$  were calculated in [26], but only for the value  $(A, B) = (0, 1)$ . We claim that these are isomorphic to our Ext groups as the two complexes

$$\mathcal{O} \xrightarrow{A\alpha_1+B\alpha_2} \mathcal{O}(1), \quad (4.56)$$

$$\mathcal{O} \xrightarrow{\alpha_2} \mathcal{O}(1), \quad (4.57)$$

are isomorphic in  $\mathcal{D}^b(Y_+)$ . To see this consider the following automorphism of the conifold

$$f : (\alpha_1, \alpha_2, \beta_1, \beta_2) \mapsto \left( \alpha_1, \frac{1}{B}(\alpha_2 - A\alpha_1), \beta_1, \beta_2 \right) \equiv (\tilde{\alpha}_1, \tilde{\alpha}_2, \beta_1, \beta_2). \quad (4.58)$$

Observe that  $A\tilde{\alpha}_1 + B\tilde{\alpha}_2 = \alpha_2$ . One readily checks that

$$\begin{array}{ccc} f^*\mathcal{O} & \xrightarrow{A\tilde{\alpha}_1+B\tilde{\alpha}_2} & f^*\mathcal{O}(1) \\ \downarrow \cong & & \downarrow \cong \\ \mathcal{O} & \xrightarrow{\alpha_2} & \mathcal{O}(1). \end{array} \quad (4.59)$$

Similarly, we obtain an isomorphism

$$\begin{array}{ccc} g^*\mathcal{O}(-1) & \xrightarrow{A\tilde{\beta}_1+B\tilde{\beta}_2} & g^*\mathcal{O} \\ \downarrow \cong & & \downarrow \cong \\ \mathcal{O}(-1) & \xrightarrow{\beta_2} & \mathcal{O}, \end{array} \quad (4.60)$$

where

$$g : (\alpha_1, \alpha_2, \beta_1, \beta_2) \mapsto \left( \alpha_1, \alpha_2, \beta_1, \frac{1}{B}(\beta_2 - A\beta_1) \right) \equiv (\alpha_1, \alpha_2, \tilde{\beta}_1, \tilde{\beta}_2). \quad (4.61)$$

This implies that all Ext groups computed in [26] are isomorphic to the ones we will need, e.g.

$$\text{Ext}^j(F_0, F_1) \cong (0, \mathbb{C}[\alpha_1\beta_1], 0, 0), \quad (4.62)$$

$$\text{Ext}^j(F_1, F_0) \cong (0, \mathbb{C}[\beta_1\alpha_1], 0, 0). \quad (4.63)$$

#### 4.2.2 The non-flat point at weak coupling

We now describe the relevant branes in our setup. There are the three pairs of objects

$$F_0^i = \mathcal{O} \xrightarrow{A^i\alpha_1+B^i\alpha_2} \mathcal{O}(1) \in \text{Obj}(\mathcal{D}^b(Y_+)) \quad (4.64)$$

$$F_1^i = \mathcal{O} \xrightarrow{A^i\beta_1+B^i\beta_2} \mathcal{O}(-1) \in \text{Obj}(\mathcal{D}^b(Y_+)). \quad (4.65)$$

These correspond to D7 branes located at the **5** curve. Moreover there is one pair of objects corresponding to D7 branes coming from the **10** curve

$$G_0 = \mathcal{O} \xrightarrow{\alpha_1} \mathcal{O}(1) \in \text{Obj}(\mathcal{D}^b(Y_+)) \quad (4.66)$$

$$G_1 = \mathcal{O} \xrightarrow{\beta_1} \mathcal{O}(-1) \in \text{Obj}(\mathcal{D}^b(Y_+)). \quad (4.67)$$

We also have fractional branes D(-1) instantons described by objects  $I_0 = S_0[-1]$  and  $I_1 = S_1[-1]$  where

$$S_0 = \mathcal{O}(2) \xrightarrow{\begin{pmatrix} \beta_2 \\ -\beta_1 \end{pmatrix}} \mathcal{O}(1)^{\oplus 2} \xrightarrow{(\beta_1, \beta_2)} \mathcal{O} \in \text{Obj}(\mathcal{D}^b(Y_+)) \quad (4.68)$$

$$S_1 = \mathcal{O}(1) \xrightarrow{\begin{pmatrix} -\beta_2 \\ \beta_1 \end{pmatrix}} \mathcal{O}^{\oplus 2} \xrightarrow{(\beta_1, \beta_2)} \mathcal{O}(-1) \longrightarrow 0 \quad (4.69)$$

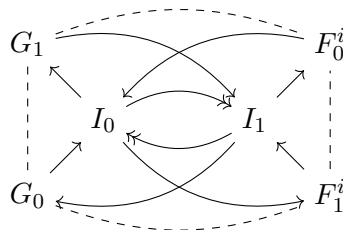


**Figure 3.** Quiver theory for GUT and flavor branes. Note that one should draw  $F_0^1, F_0^2, F_0^3$  separately and connect to the other nodes as indicated. For the sake of clarity only one flavor brane/image brane is shown.

A computation of the Ext groups shows [26]

$$\text{Ext}^i(G_0, I_0) = (0, \mathbb{C}, 0, 0), \quad \text{Ext}^i(G_0, I_1) = (0, 0, \mathbb{C}, 0) \quad (4.70)$$

$$\text{Ext}^i(G_1, I_0) = (0, 0, \mathbb{C}, 0), \quad \text{Ext}^i(G_1, I_1) = (0, \mathbb{C}, 0, 0) \quad (4.71)$$

$$\text{Ext}^i(F_0, I_0) = (0, \mathbb{C}, 0, 0), \quad \text{Ext}^i(F_0, I_1) = (0, 0, \mathbb{C}, 0) \quad (4.72)$$

$$\text{Ext}^i(F_1, I_0) = (0, 0, \mathbb{C}, 0), \quad \text{Ext}^i(F_1, I_1) = (0, \mathbb{C}, 0, 0), \quad (4.73)$$

and

$$\text{Ext}^i(G_0, G_1) \cong (0, \mathbb{C}[\alpha_2\beta_2], 0, 0), \quad \text{Ext}^i(G_0, F_1) \cong (0, \mathbb{C}[\alpha_1\beta_2], 0, 0) \quad (4.74)$$

$$\text{Ext}^i(G_1, G_0) \cong (0, \mathbb{C}[\beta_2\alpha_2], 0, 0), \quad \text{Ext}^i(G_1, F_0) \cong (0, \mathbb{C}[\beta_1\alpha_2], 0, 0) \quad (4.75)$$

$$\text{Ext}^i(F_0, F_1) \cong (0, \mathbb{C}[\alpha_1\beta_1], 0, 0), \quad \text{Ext}^i(F_0, G_1) \cong (0, \mathbb{C}[\alpha_2\beta_1], 0, 0) \quad (4.76)$$

$$\text{Ext}^i(F_1, F_0) \cong (0, \mathbb{C}[\beta_1\alpha_1], 0, 0), \quad \text{Ext}^i(F_1, G_0) \cong (0, \mathbb{C}[\beta_2\alpha_1], 0, 0). \quad (4.77)$$

Also we have

$$\text{Ext}^1(I_1, I_0) \cong \text{Ext}^1(I_0, I_1) \cong \mathbb{C}^2. \quad (4.78)$$

This situation is neatly summarized in a quiver diagram shown in figure 3.

In order to obtain the desired theory after orientifolding one takes the branes  $G_i$  with multiplicity 5 to generate the GUT stack. A chiral bifundamental string between  $G_0$  and  $G_1$  giving rise to a state in the  $\mathbf{10}$  representation upon orientifolding. This can be derived more rigorously by considering the gauge group on empty nodes. In [26] it was shown that indeed we obtain  $USp(0)$ .

The flavor branes  $F_j^i$  are each chosen with multiplicity 1. Between  $G_1$  and each  $F_0^j$  we have a bifundamental with the same chirality as above giving rise to a  $\mathbf{5}$  state. Instanton effects arise from D1 branes wrapping the nodes  $I_i$ . We will only consider the case of a single instanton.

Firstly, consider a D1 brane wrapping  $I_1$ . This gives rise to charged zero modes as in figure 4. Hence, the superpotential reads

$$W_{\text{inst}} = \lambda_1^i \mathbf{10}^{[ij]} \lambda_1^j + \lambda_1^i ((\mathbf{5}^1)^i \nu_{11} + (\mathbf{5}^2)^i \nu_{12} + (\mathbf{5}^3)^i \nu_{13}). \quad (4.79)$$

Performing the integral

$$\int d\lambda_1^i d\nu_{11} d\nu_{12} d\nu_{13} \exp(W_{\text{inst}}) = \mathbf{10} \mathbf{5}^1 \mathbf{5}^2 \mathbf{5}^3, \quad (4.80)$$

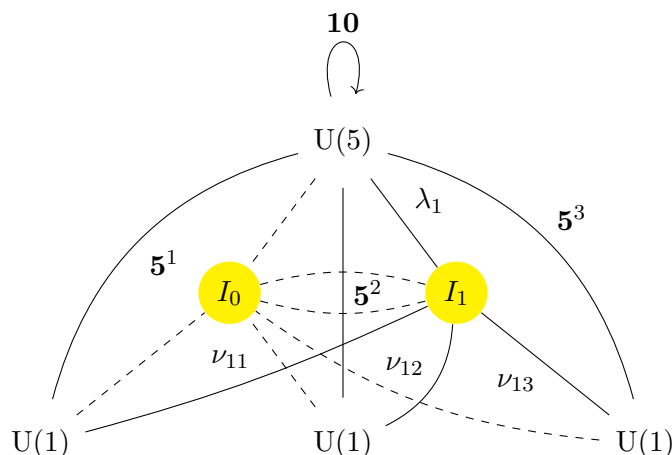


**Figure 4.** Relevant zero modes for one D1 brane wrapping  $I_1$  after orientifolding. Dashed lines indicate possible string states, but since  $I_0$  is not occupied they play no relevance here. Labels such as  $\nu_{12}$  refer only to bold lines. Note that we have orientifolded the quiver shown above.

we obtain the desired coupling. If on the other hand we wrap one D1 brane around the  $I_0$  node, there will be no contribution to the superpotential due to our choice of chirality.

### 5 The mirror picture

Finally, it is interesting to see how the superpotential coupling appears from the mirror IIA perspective. This mirror picture gives a useful heuristic understanding of the physics, but the analysis is harder to make fully precise than in the IIB setting, where we have a well defined problem in algebraic geometry. The analysis is very similar to that in [26] (building on previous work in [37–39]), so we will be somewhat brief.

For the purposes of computing holomorphic data the topology of the mirror to the conifold can be described by a fibration over  $\mathbb{C}$  with fiber  $\mathbb{C}^* \times \Sigma$  [40, 41], described by

$$\begin{aligned} uv &= W, \\ P(x, y) &= W, \end{aligned} \tag{5.1}$$

where  $W \in \mathbb{C}$  parameterizes the base of the fibration,  $u, v \in \mathbb{C}$  parameterize the  $\mathbb{C}^*$  fiber, and  $x, y \in \mathbb{C}^*$  describe the (punctured) Riemann surface  $\Sigma$ . For the specific case of the conifold, we can choose a framing [42] such that

$$P(x, y) = q + x + y + xy - xy^2. \tag{5.2}$$

Here  $q$  is a complex structure modulus mirror to the complexified size of the small resolution of the conifold. This equation defines a  $\mathbb{P}^1$  punctured at four points. As discussed in detail in [37], for the purposes of computing holomorphic quiver data for our system, it is enough to focus our attention on  $\Sigma$ .

In addition to the geometric background itself, we need to describe how the branes wrap the geometry. The case with one U(5) stack and one additional U(1) brane stack was

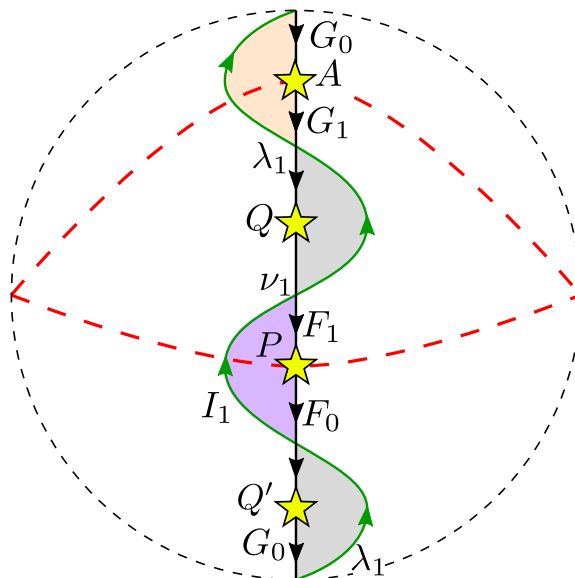


**Figure 5.** Structure of branes and the orientifold involution on  $\Sigma$ . The outer dashed line should be identified with a point to obtain  $\mathbb{P}^1$ . The four punctures have been marked by stars, and the orientifold involution induces a reflection along the red line (which becomes a reflection along the equator on  $\mathbb{P}^1$ ).

described in detail in [26]. An important difference in our case is that, in addition to the U(5) stack, we have *three* U(1) flavor branes. We will start by analyzing the case in which all U(1) branes are coincident, leading to a flavor stack with gauge group  $U(3) \times U(5)$ . The restriction of the brane system to  $\Sigma$  can then be determined by identical arguments to those in [26], with the result shown in figure 5.

There are various features to note in figure 5. We have the  $G_0 \sim G_1$  stacks (the identification is due to the orientifold action), associated with the U(5) stack, and the  $F_0 \sim F_1$  stacks, associated to U(3). We obtain various fields, as these stacks intersect each other,<sup>11</sup> and additional matter fields as the flavor stacks intersect the instanton brane  $I_1$ , with gauge group  $O(1) = \mathbb{Z}_2$ . The resulting matter content can be summarized as

	U(5)	U(3)	O(1)	
A	<b>10</b>	<b>1</b>	0	.
Q	<b>5</b>	<b><math>\bar{3}</math></b>	0	
P	<b>1</b>	<b>3</b>	0	
λ	<b><math>\bar{5}</math></b>	<b>1</b>	1	
ν	<b>1</b>	<b>3</b>	1	

Note that  $P$  is most naturally the (complex conjugate of the) two-index representation of SU(3), which can be identified with the fundamental representation. The worldsheet instantons depicted in figure 5 then generate an effective action for the charged instanton

<sup>11</sup>Since the intersection is at a puncture, the existence of massless matter associated with the “intersection” is external input data from the point of view of the theory at the singularity.

zero modes of the form

$$S_{\text{inst}} = \lambda^i Q_i^a \nu_a + \lambda^i A_{[ij]} \lambda^j + \nu_a P^{[ab]} \nu_b \tag{5.4}$$

where raising the index corresponds to going to the complex conjugate representation. The effective non-perturbative superpotential one obtains from integrating out the charged zero modes is then of the form

$$W_{\text{np}} = \varepsilon_{abc} \varepsilon^{ijklm} A_{[ij]} Q_k^a Q_l^b Q_m^c + \varepsilon_{abc} \varepsilon^{ijklm} A_{[ij]} A_{[kl]} Q_m^a P^{[bc]} \cong AQ^3 + A^2PQ \tag{5.5}$$

where we have omitted the unknown (but generically nonzero, since the relevant worldsheet instantons have generically finite area) coefficients of the various terms in the superpotential, which depend on various geometric and brane moduli.

It is now a simple job to deform away from the  $U(3)$  locus. This can be seen as a Higgsing of the  $SU(3)$  flavor symmetry, which will give a mass to at least some of the fields in  $P$ , and generically to all of them.<sup>12</sup> We can model this as the deformation of (5.5) given by

$$W_{\text{np}} \rightarrow AQ^3 + A^2PQ + mP^2, \tag{5.6}$$

where, for simplicity, we have set all of the masses equal. Integrating out  $P$  then leads to an effective superpotential of the form

$$W'_{\text{np}} = AQ^3 - \frac{1}{4m} (QA^2)^2 \tag{5.7}$$

which in the  $m \rightarrow \infty$  limit leads to the superpotential that we have argued for in the previous section.

## 6 Conclusions

The main focus of this note has been to understand non-flat fibres, in co-dimension three, in F-theory and, in particular, their effect on the low-energy dynamics. In previous analyses of the models that we discuss here, this issue was sidestepped by drastically restricting the base manifolds under consideration. Here we tied up this loose end, by showing that it is not necessary to restrict the base manifolds to avoid these points, as they are harmless for the good phenomenological properties of the model.

Although we concentrated on one specific model for concreteness, it is clear that the conclusions should hold fairly generally. This result is significant for F-theory model building because non-flat points seem to appear rather frequently. Hence, our result, that they are harmless, does away with the need of having to worry about choosing the base of the fibration with care in order to avoid such points, and simplifies model building.

---

<sup>12</sup>We will nevertheless keep the  $Q$  fields massless. Recall from footnote 11 that the massless spectrum of GUT fields is external data from the point of view of the singularity, which will be determined by global considerations.

## Acknowledgments

C.M. would like to thank Ling Lin, Eran Palti and Timo Weigand for discussions and collaboration on a related project. The research of I.A. was supported by the IMPRS program of the MPP Munich and C.M. was funded in part by the Munich Excellence Cluster for Fundamental Physics “Origin and the Structure of the Universe”.

## A 6d anomaly cancellation

We now verify the anomaly cancellation condition for the  $\mathbb{Q}$ -factorial Calabi-Yau threefolds with terminal singularities of section 2. As is very well explained in [16] a  $\mathbb{Q}$ -factorial variety  $X$  is one where for each Weil divisor  $D$  there exist an integer  $n$  such that  $nD$  is Cartier. If the resolved variety  $\tilde{X}$  has canonical class  $\tilde{K}$  and  $X$  has canonical class  $K$  then under the given circumstance

$$n\tilde{K} = f^*(nK) + n \sum a_i E_i, \tag{A.1}$$

for some integers  $n, a_i$ . Here  $E_i$  are classes of the exceptional divisors. If  $a_i > 0$  for all  $i$ , then the singularities are called terminal.

Physically these singularities imply a localization of matter states from wrapped M2-branes, that is a number of uncharged hyper multiplets.

To verify the anomaly cancellation condition we have to compute the number of tensor, vector and hyper multiplets,  $n_T, n_V, n_H$  arising from such a compactification. These have to satisfy

$$29n_T - n_V + n_H = 273. \tag{A.2}$$

We know that since we have an  $SU(5) \times U(1)$  matter group

$$n_T = 0, \quad n_V = 24 + 1 = 25. \tag{A.3}$$

This leaves us with an unknown number of hyper multiplets  $n_H$ . As is well known these number splits up into number of uncharged  $n_H^0$  and charged hyper multiplets  $n_H^c$

$$n_H = n_H^0 + n_H^c. \tag{A.4}$$

The charged hyper multiplets  $n_H^c$  are counted by algebro-geometric means, and  $n_H^0$  is computed via the topology of our variety.

### A.1 Counting charged hyper multiplets

Charged hyper multiplets arise from so-called matter loci associated to gauge groups present in our theory. In the case at hand we have several charge **10** and charge **5** loci as well as singlets.

We now restrict ourselves to working with

$$n = \deg(\delta) = 2, \quad \deg(\alpha) = 1, \tag{A.5}$$

which yields

$$\begin{aligned}
[\alpha] &\Rightarrow \deg(\alpha) = 1 \\
[\beta] &= c_1(B_2) + [\delta] - [\omega] \Rightarrow \deg(\beta) = 4 \\
[\gamma] &= 4c_1(B_2) - 2[\delta] - 3[\omega] - [\alpha] \Rightarrow \deg(\gamma) = 4 \\
[\delta] &\Rightarrow \deg(\delta) = 2 \\
[c_2] &= [\delta] + [\alpha] + [\omega] - c_1(B_2) \Rightarrow \deg(c_2) = 1 \\
[d_2] &= 3c_1(B_2) - [\delta] - 2[\omega] - [\alpha] \Rightarrow \deg(d_2) = 4 \\
[d_3] &= 2c_1(B_2) - [\delta] - [\alpha] - [\omega] \Rightarrow \deg(d_3) = 2.
\end{aligned}$$

Here we exploit the fact that over  $B_2 = \mathbb{P}^2$  the degree of a homogenous ploynomial is equal to the first Chern class of its associated line bundle. The charge **10** states are located at (2.16). It follows from Bezouts theorem that there are  $\deg(\omega) \cdot (\deg(d_3) + \deg(c_2)) = 3$  such points on the base. This gives us 30 hyper multiplets.

The charge **5** loci are given by (2.17). Applying Bezouts theorem again yields a total of  $2 + 6 + 11 = 19$  such points. This gives a contribution of  $5 \cdot 19 = 95$  multiplets.

Counting the number of singlets is more involved. We know [15] that the singlets of U(1) charge  $\pm 10$  are located at

$$\delta = \omega\beta - \frac{1}{2}c_2d_3\delta = 0. \tag{A.6}$$

This is equivalent to

$$\delta = \beta = 0. \tag{A.7}$$

In our specific case Bezouts theorem implies that there are

$$\deg(\delta) \cdot \deg(\beta) = 2 \cdot 4 = 8, \tag{A.8}$$

such points.

The singlets of U(1) charge  $\pm 5$  are located at the points satisfying

$$\begin{aligned}
F_1 := & \beta c_2^2 d_3^2 \delta^2 + c_2^2 d_2 d_3 \delta^3 - 3\beta^2 c_2 d_3 \delta \omega - 2\beta c_2 d_2 \delta^2 \omega \\
& + \gamma c_2 \delta^4 \omega + \alpha \beta d_3 \delta^3 \omega + \alpha d_2 \delta^4 \omega + 2\beta^3 \omega^2 = 0,
\end{aligned} \tag{A.9}$$

$$\begin{aligned}
F_2 := & -\alpha \beta c_2 d_3^2 \delta^4 - \alpha c_2 d_2 d_3 \delta^5 + \beta^2 c_2^2 d_3^2 \delta^2 \\
& + 2\beta c_2^2 d_2 d_3 \delta^3 + c_2^2 d_2^2 \delta^4 - 2\beta^3 c_2 d_3 \delta \omega \\
& - 2\beta^2 c_2 d_2 \delta^2 \omega + \alpha \beta^2 d_3 \delta^3 \omega + \beta^4 \omega^2 - \alpha \gamma \delta^6 \omega = 0.
\end{aligned} \tag{A.10}$$

In addition points satisfying one of the following conditions must be excluded from this list:

$$\begin{aligned}
\delta &= \beta = 0 \\
\delta d_2 + \beta d_3 &= 0 \\
c_2 &= \omega = 0 \\
\delta &= \omega = 0.
\end{aligned} \tag{A.11}$$

Generically the locus  $F_1 = F_2 = 0$  consists of  $14 \cdot 18$  points. We now subtract the points of (A.11) weighted by their proper intersection multiplicity. This yields

$$14 \cdot 18 - 16 \cdot 2 \cdot 4 - 2 \cdot 6 - 1 \cdot 1 \cdot 1 - 10 \cdot 2 \cdot 1 = 91. \tag{A.12}$$

All in all the number of uncharged hyper multiplets is

$$30 + 95 + 8 + 91 = 224. \tag{A.13}$$

## A.2 Counting uncharged hyper multiplets

The number of uncharged hyper multiplets is computed from the topological Euler characteristic and  $h^{1,1}$  of our variety. We know that

$$h^{1,1} = 6. \tag{A.14}$$

Strictly speaking this is the Hodge number of a smooth threefold rationally equivalent to our singular variety. The existence of such a deformation is guaranteed by [23].

The Euler characteristic of the singular variety is computed by first computing it for a smooth representative of its rational equivalence class. Then we use the fact that [43]

$$\chi(X_{\text{Sing}}) - \chi(X_{\text{smooth}}) = \sum_P m_P, \tag{A.15}$$

where the latter sum runs over the singular points  $P$  and  $m_P$  denotes the Milnor number of such a point.

The Euler characteristic  $\chi(X_{\text{smooth}})$  is computed using the toric embedding and turns out to be

$$\chi(X_{\text{smooth}}) = -132. \tag{A.16}$$

We know that there is only one type of singularity located at

$$\alpha = \gamma = 0, \tag{A.17}$$

which are  $1 \cdot 4 = 4$  points. The Milnor numbers turn out to be

$$m_P = 2. \tag{A.18}$$

We thus end up with

$$\chi(X_{\text{Sing}}) = \chi(X_{\text{smooth}}) + \sum_P m_P = -124. \tag{A.19}$$

The number of uncharged multiplets then is simply

$$n_H^0 = 1 + h^{1,1} - \frac{1}{2}\chi(X_{\text{sing}}) + \frac{1}{2}\sum_P m_P = 7 + 62 + 4 = 73. \tag{A.20}$$

We now add the universal hyper multiplet to that number to end up with

$$1 + n_H^0 = 74. \tag{A.21}$$

We see that the anomaly cancellation condition is satisfied by computing

$$1 + n_H^0 + n_H^c - n_V = 1 + 73 + 224 - 25 = 273. \tag{A.22}$$

**Open Access.** This article is distributed under the terms of the Creative Commons Attribution License ([CC-BY 4.0](https://creativecommons.org/licenses/by/4.0/)), which permits any use, distribution and reproduction in any medium, provided the original author(s) and source are credited.

## References

- [1] C. Vafa, *Evidence for F-theory*, *Nucl. Phys. B* **469** (1996) 403 [[hep-th/9602022](#)] [[INSPIRE](#)].
- [2] R. Donagi and M. Wijnholt, *Model Building with F-theory*, *Adv. Theor. Math. Phys.* **15** (2011) 1237 [[arXiv:0802.2969](#)] [[INSPIRE](#)].
- [3] C. Beasley, J.J. Heckman and C. Vafa, *GUTs and Exceptional Branes in F-theory — I*, *JHEP* **01** (2009) 058 [[arXiv:0802.3391](#)] [[INSPIRE](#)].
- [4] H. Hayashi, R. Tatar, Y. Toda, T. Watari and M. Yamazaki, *New Aspects of Heterotic-F Theory Duality*, *Nucl. Phys. B* **806** (2009) 224 [[arXiv:0805.1057](#)] [[INSPIRE](#)].
- [5] C. Beasley, J.J. Heckman and C. Vafa, *GUTs and Exceptional Branes in F-theory — II: Experimental Predictions*, *JHEP* **01** (2009) 059 [[arXiv:0806.0102](#)] [[INSPIRE](#)].
- [6] R. Donagi and M. Wijnholt, *Breaking GUT Groups in F-theory*, *Adv. Theor. Math. Phys.* **15** (2011) 1523 [[arXiv:0808.2223](#)] [[INSPIRE](#)].
- [7] E. Witten, *Phase transitions in M-theory and F-theory*, *Nucl. Phys. B* **471** (1996) 195 [[hep-th/9603150](#)] [[INSPIRE](#)].
- [8] P. Candelas, D.-E. Diaconescu, B. Florea, D.R. Morrison and G. Rajesh, *Codimension three bundle singularities in F-theory*, *JHEP* **06** (2002) 014 [[hep-th/0009228](#)] [[INSPIRE](#)].
- [9] V. Braun, T.W. Grimm and J. Keitel, *New Global F-theory GUTs with U(1) symmetries*, *JHEP* **09** (2013) 154 [[arXiv:1302.1854](#)] [[INSPIRE](#)].
- [10] J. Borchmann, C. Mayrhofer, E. Palti and T. Weigand, *SU(5) Tops with Multiple U(1)s in F-theory*, *Nucl. Phys. B* **882** (2014) 1 [[arXiv:1307.2902](#)] [[INSPIRE](#)].
- [11] V. Bouchard and H. Skarke, *Affine Kac-Moody algebras, CHL strings and the classification of tops*, *Adv. Theor. Math. Phys.* **7** (2003) 205 [[hep-th/0303218](#)] [[INSPIRE](#)].
- [12] V. Braun, T.W. Grimm and J. Keitel, *Geometric Engineering in Toric F-theory and GUTs with U(1) Gauge Factors*, *JHEP* **12** (2013) 069 [[arXiv:1306.0577](#)] [[INSPIRE](#)].
- [13] J. Marsano, N. Saulina and S. Schäfer-Nameki, *Compact F-theory GUTs with U(1) (PQ)*, *JHEP* **04** (2010) 095 [[arXiv:0912.0272](#)] [[INSPIRE](#)].
- [14] M.J. Dolan, J. Marsano, N. Saulina and S. Schäfer-Nameki, *F-theory GUTs with U(1) Symmetries: Generalities and Survey*, *Phys. Rev. D* **84** (2011) 066008 [[arXiv:1102.0290](#)] [[INSPIRE](#)].
- [15] C. Mayrhofer, E. Palti and T. Weigand, *U(1) symmetries in F-theory GUTs with multiple sections*, *JHEP* **03** (2013) 098 [[arXiv:1211.6742](#)] [[INSPIRE](#)].
- [16] P. Arras, A. Grassi and T. Weigand, *Terminal Singularities, Milnor Numbers and Matter in F-theory*, *J. Geom. Phys.* **123** (2018) 71 [[arXiv:1612.05646](#)] [[INSPIRE](#)].
- [17] M. Bies, C. Mayrhofer and T. Weigand, *Gauge Backgrounds and Zero-Mode Counting in F-theory*, *JHEP* **11** (2017) 081 [[arXiv:1706.04616](#)] [[INSPIRE](#)].
- [18] M. Dierigl, P.-K. Oehlmann and F. Ruehle, *Global Tensor-Matter Transitions in F-Theory*, *Fortsch. Phys.* **66** (2018) 1800037 [[arXiv:1804.07386](#)] [[INSPIRE](#)].

- [19] D.R. Morrison and C. Vafa, *Compactifications of F-theory on Calabi-Yau threefolds. 1*, *Nucl. Phys. B* **473** (1996) 74 [[hep-th/9602114](#)] [[INSPIRE](#)].
- [20] D.R. Morrison and D.S. Park, *F-Theory and the Mordell-Weil Group of Elliptically-Fibered Calabi-Yau Threefolds*, *JHEP* **10** (2012) 128 [[arXiv:1208.2695](#)] [[INSPIRE](#)].
- [21] D. Klevers, D.K. Mayorga Pena, P.-K. Oehlmann, H. Piragua and J. Reuter, *F-Theory on all Toric Hypersurface Fibrations and its Higgs Branches*, *JHEP* **01** (2015) 142 [[arXiv:1408.4808](#)] [[INSPIRE](#)].
- [22] A. Grassi and T. Weigand, *On topological invariants of algebraic threefolds with ( $\mathbb{Q}$ -factorial) singularities*, [arXiv:1804.02424](#) [[INSPIRE](#)].
- [23] Y. Namikawa and J.H.M. Steenbrink, *Global smoothing of calabi-yau threefolds*, *Invent. Math.* **122** (1995) 403.
- [24] E. Witten, *On flux quantization in M-theory and the effective action*, *J. Geom. Phys.* **22** (1997) 1 [[hep-th/9609122](#)] [[INSPIRE](#)].
- [25] D.S. Freed and E. Witten, *Anomalies in string theory with D-branes*, *Asian J. Math.* **3** (1999) 819 [[hep-th/9907189](#)] [[INSPIRE](#)].
- [26] A. Collinucci and I. García-Etxebarria,  *$E_6$  Yukawa couplings in F-theory as D-brane instanton effects*, *JHEP* **03** (2017) 155 [[arXiv:1612.06874](#)] [[INSPIRE](#)].
- [27] M. Bies, C. Mayrhofer, C. Pehle and T. Weigand, *Chow groups, Deligne cohomology and massless matter in F-theory*, [arXiv:1402.5144](#) [[INSPIRE](#)].
- [28] T.W. Grimm and T. Weigand, *On Abelian Gauge Symmetries and Proton Decay in Global F-theory GUTs*, *Phys. Rev. D* **82** (2010) 086009 [[arXiv:1006.0226](#)] [[INSPIRE](#)].
- [29] S. Krause, C. Mayrhofer and T. Weigand,  *$G_4$  flux, chiral matter and singularity resolution in F-theory compactifications*, *Nucl. Phys. B* **858** (2012) 1 [[arXiv:1109.3454](#)] [[INSPIRE](#)].
- [30] T. Shioda, *Mordell-Weil Lattices and Galois Representation. I*, *Proc. Japan Acad. A* **65** (1989) 268.
- [31] R. Wazir, *Arithmetic on elliptic threefolds*, *Compos. Math.* **140** (2004) 567 [[math.NT/0112259](#)].
- [32] D.S. Park, *Anomaly Equations and Intersection Theory*, *JHEP* **01** (2012) 093 [[arXiv:1111.2351](#)] [[INSPIRE](#)].
- [33] J. Tate, *Algorithm for determining the type of a singular fiber in an elliptic pencil*, Springer Berlin Heidelberg, (1975), pp. 33–52.
- [34] A. Sen, *Orientifold limit of F-theory vacua*, *Phys. Rev. D* **55** (1997) R7345 [[hep-th/9702165](#)] [[INSPIRE](#)].
- [35] M. Van den Bergh, *Non-commutative crepant resolutions*, [math/0211064](#).
- [36] P.S. Aspinwall, *D-branes on Calabi-Yau manifolds*, in *Progress in string theory. Proceedings, Summer School, TASI 2003, Boulder, U.S.A., June 2–27, 2003*, pp. 1–152, 2004, [hep-th/0403166](#), DOI [[INSPIRE](#)].
- [37] B. Feng, Y.-H. He, K.D. Kennaway and C. Vafa, *Dimer models from mirror symmetry and quivering amoebae*, *Adv. Theor. Math. Phys.* **12** (2008) 489 [[hep-th/0511287](#)] [[INSPIRE](#)].
- [38] D. Forcella, I. García-Etxebarria and A. Uranga,  *$E3$ -brane instantons and baryonic operators for  $D3$ -branes on toric singularities*, *JHEP* **03** (2009) 041 [[arXiv:0806.2291](#)] [[INSPIRE](#)].

- [39] S. Franco and A. Uranga, *Bipartite Field Theories from D-branes*, *JHEP* **04** (2014) 161 [[arXiv:1306.6331](#)] [[INSPIRE](#)].
- [40] K. Hori and C. Vafa, *Mirror symmetry*, [hep-th/0002222](#) [[INSPIRE](#)].
- [41] K. Hori, A. Iqbal and C. Vafa, *D-branes and mirror symmetry*, [hep-th/0005247](#) [[INSPIRE](#)].
- [42] V. Bouchard and P. Sulkowski, *Topological recursion and mirror curves*, *Adv. Theor. Math. Phys.* **16** (2012) 1443 [[arXiv:1105.2052](#)] [[INSPIRE](#)].
- [43] W. Fulton, *Intersection Theory*, Princeton University Press, (1993).